Heterobimetallic Aggregates of Copper(I) with Thio-tungstate and -molybdate. Cation Effect in Aggregation of $MS_4Cu_4Cl_4$ Units, a Crystallographic Study†

Francis Sécheresse,* Sylvain Bernés, Francis Robert and Yves Jeannin
Laboratoire de Chimie des Métaux de Transition, URA-CNRS 419, Université Pierre et Marie Curie, 4 place Jussieu, 75252 Paris Cédex 05, France

Reaction of $[MS_4]^{2-}$ (M = Mo or W) with CuCl in dichloromethane or acetonitrile gives a new set of bimetallic compounds isolated with various geometries for the same 1:4:4 M:S:Cu composition. Crystals of $[NBu_4]_2[MoS_4Cu_4Cl_4]$ **1a** are tetragonal, space group $I\bar{4}/m$, $a = 13.343(5)$, $c = 14.113(2)$ Å, $Z = 2$, $R = 0.058$. The crystal structure reveals discrete $[MoS_4Cu_4Cl_4]^{2-}$ anions separated in the lattice by $[NBu_4]^+$ cations. The isostructural tungsten homologue **1b** was isolated and characterized: space group $I\bar{4}/m$, tetragonal, $a = 13.342(4)$, $c = 14.106(5)$ Å. The structure of $[PPh_4][NPr_4][MoS_4Cu_4Cl_4]$ **2** consists of a dimeric aggregate: monoclinic, space group $P2_1/n$, $a = 9.962(8)$, $b = 36.951(5)$, $c = 13.114(3)$ Å, $\beta = 105.71(6)°$, $R = 0.056$. The salt $[NPr_4]_2[WS_4Cu_4Cl_4]$ **3b** is polymerized through linear chains. Crystals are triclinic, space group $P\bar{1}$, $a = 10.283(1)$, $b = 13.925(1)$, $c = 15.245(1)$ Å, $\alpha = 110.32(1)$, $\beta = 90.64(1)$, $\gamma = 102.49(1)°$, $Z = 2$, $R = 0.031$. The isostructural molybdenum compound **3a** was also characterized: triclinic, $a = 10.275$, $b = 13.961$, $c = 15.270$ Å, $\alpha = 110.57$, $\beta = 90.70$, $\gamma = 102.30°$. The arrangements of the mono-, di- and poly-meric aggregates in the lattice are discussed in terms of the size of the counter anion. For compounds **1b** and **3a** only the cell dimensions were determined.

Neutral derivatives of copper(I), CuCN, CuCl and CuNCS, are co-ordinated easily by the tetrathiometalates $[MS_4]^{2-}$ (M = Mo or W).[1–5] Owing to the high tendency of Cu^I to form metal–sulphur bonds and the versatility of the $[MS_4]^{2-}$ ligands, a large set of compounds resulting from the progressive saturation of the six edges of the MS_4 tetrahedron can be obtained. With copper cyanide the dianion $[WS_4(CuCN)_2]^{2-}$ was isolated in the solid state as discrete units with the counter cations $[PPh_4]^+$ (ref. 1*a*) or $[NPr_4]^+$,[1b] and with the cation $[NMe_4]^+$,[1a] as polymeric zigzag chains. With copper chloride, $[WS_4(CuCl)_2]^{2-}$,[2] $[WS_4(CuCl)_3]^{2-}$,[3] $[MoS_4(CuCl)_3]^{2-}$ (ref. 4) and $[WS_4(CuCl)_5Cl_2]^{4-}$ (ref. 5) were structurally characterized as discrete anions. In contrast, $[MoS_4(CuBr)_4]^{2-}$ (ref. 6) contains polymeric anion chains and $[WS_4(CuCl)_4]^{2-}$ dimeric units.[7] With copper thiocyanate, owing to the ambidentate nature of the NCS^-, a set of one-, two- and three-dimensional polymerized compounds were isolated.[8–10] The dimensionality of these compounds was clearly dependent on the size of the cation associated with the polyanionic structure, three- with $[NMe_4]^+$, two- with $[NEt_4]^+$ and one-dimensional with $[PPh_4]^+$.

In this work we report another effect of the size of the counter cation on the preparation of discrete or polymeric structures: the dianion $[MS_4Cu_4Cl_4]^{2-}$ (M = Mo or W) was successfully isolated and characterized as mono-, di- and polymeric units in the solid state.

Experimental

All manipulations were carried out in air. Chemicals were used as purchased and usual solvents were obtained from commercial sources and generally used as received. Infrared spectra were recorded on a 580B Perkin-Elmer spectrophotometer (KBr pellets) and electronic spectra on a Kontron 810 spectrophotometer in dimethylformamide (dmf) solution between 600 and 250 nm. Elemental analysis were performed by the Service Central d'Analyses du CNRS.

Preparations.—$[NBu_4]_2[MoS_4Cu_4Cl_4]$ **1a**. Copper(I) chloride (150 mg, 1.5 mmol) was added to a solution of $[NBu_4]_2[MoS_4]$ (177 mg, 0.25 mmol) in dichloromethane (30 cm^3) and the resulting red solution refluxed for 48 h. After elimination of a black solid, Et_2O (15 cm^3) was layered upon the red filtrate and the mixture allowed to stand at room temperature. Within 1 h red crystals formed, and were filtered off and dried (60 mg, yield 22%) [Found (Calc. for $C_{32}H_{72}Cl_4Cu_4MoN_2S_4$): C, 35.10 (34.80); H, 6.85 (6.50); Cl, 12.75 (12.85); Cu, 22.30 (23.00); Mo, 8.80 (8.70); N, 2.60 (2.55); S, 11.75 (11.60%)].

$[NBu_4]_2[WS_4Cu_4Cl_4]$ **1b**. The salt $[NBu_4]_2[WS_4]$ (200 mg, 0.25 mmol) was dissolved in dichloromethane (30 cm^3). To this solution was added with stirring copper(I) chloride (150 mg, 1.5 mmol) and the mixture refluxed for 45 min. After elimination of a red precipitate, addition of Et_2O (10 cm^3) to the filtrate and storage for 12 h at 20 °C afforded yellow crystals (80 mg, yield 27%) [Found (Calc. for $C_{32}H_{72}Cl_4Cu_4N_2S_4W$): C, 32.00 (32.20); H, 6.25 (6.05); Cl, 12.00 (11.90); Cu, 21.40 (21.30); N, 2.25 (2.35); S, 11.04 (10.75); W, 15.10 (15.45%)].

$[PPh_4][NPr_4][MoS_4Cu_4Cl_4]$ **2**. The salt $[PPh_4]_2[MoS_4(CuCl)_3]$ (145 mg, 0.12 mmol)[4] was dissolved in acetonitrile (30 cm^3) and treated with a solution of copper(I) chloride (36 mg, 0.36 mmol) and NPr_4Cl (80 mg, 0.36 mmol) in acetonitrile (15 cm^3). This solution was refluxed for 3 h and then cooled to room temperature. Addition of Et_2O (15 cm^3) and standing for 1 week at room temperature yielded three kinds of well shaped crystals: (*i*) dark red needles identified by complete X-ray structural determination as $C_{36}H_{48}Cl_4Cu_4MoNPS_4$ **2**, (*ii*) violet crystals identified as **3a** from cell dimensions determination and (*iii*) black platelets of $[NPr_4]_3[MoS_4(CuCl)_4Cl]$ which will be described elsewhere. The tungsten analogue of **2** was not isolated.

---

† *Supplementary data available:* see Instructions for Authors, *J. Chem. Soc., Dalton Trans.*, 1991, Issue 1, pp. xviii–xxii.

Table 1 Summary of crystallographic data[a]

Compound	**1a**	**1b**[b]	**2**	**3a**[b]	**3b**
Formula	$C_{32}H_{72}Cl_4Cu_4MoN_2S_4$	$C_{32}H_{72}Cl_4Cu_4N_2S_4W$	$C_{36}H_{48}Cl_4Cu_4MoNPS_4$	$C_{24}H_{56}Cl_4Cu_4MoN_2S_4$	$C_{24}H_{56}Cl_4Cu_4N_2S_4W$
M	1105.1	1193.0	1145.9	992.9	1080.8
Crystal system	Tetragonal	Tetragonal	Monoclinic	Triclinic	Triclinic
Space group	$I\bar{4}/m$	$I\bar{4}/m$	$P2_1/n$	$P\bar{1}$	$P\bar{1}$
a/Å	13.343(5)	13.342(4)	9.962(8)	10.275	10.283(1)
b/Å			36.951(5)	13.961	13.925(1)
c/Å	14.113(2)	14.106(5)	13.114(3)	15.270	15.245(1)
α/°				110.57	110.32(1)
β/°			105.71(6)	90.70	90.64(1)
γ/°				102.30	102.49(1)
U/Å^3	2512(1)	2510(1)	4647(75)	1995	1989(10)
Z	2	2	4	2	2
D_c/g cm^{-3}	1.46	1.58	1.64	1.65	1.80
F(000)	1136	1168	2304	1040	1072
Diffractometer	Enraf–Nonius CAD4	Enraf Nonius CAD4	Enraf Nonius CAD4	Philips PW1100	Enraf Nonius CAD4
μ/cm^{-1}	23.0		25.3		55.7
Scan type	θ–2θ		θ–2θ		θ–2θ
Scan range/°	1.0 + 0.345 tanθ		1.0 + 0.345 tanθ		1.0 + 0.345 tanθ
θ limits/°	1–25		1–25		1–25
Octants collected	$+h, +k, +l$		$\pm h, +k, +l$		$\pm h, \pm k, +l$
No. of data collected	2522		8685		7294
No. of unique reflections	1157		8160		7003
No. of reflections used	547		3684		5980
Criterion	$(F_o)^2 > 3\sigma(F_o^2)$		$(F_o)^2 > 3\sigma(F_o^2)$		$(F_o)^2 > 3\sigma(F_o^2)$
R[c]	0.058		0.056		0.031
R′[d]	0.056		0.062		0.030

[a] Details in common: Mo-Kα radiation (λ = 0.710 69 Å); graphite crystal monochromator, form factors taken from ref. 14 and secondary extinction from ref. 15. [b] Only the cell dimensions were determined. [c] $R = \Sigma(||F_o| - |F_c||)/\Sigma|F_o|$. [d] $R' = [\Sigma w(|F_o| - |F_c|)^2/\Sigma wF_o^2]^{\frac{1}{2}}$.

Table 2 Fractional atomic coordinates for $[NBu_4]_2[MoS_4Cu_4Cl_4]$ **1a**

Atom	*X*/*a*	*Y*/*b*	*Z*/*c*
Mo	0.0000	0.0000	0.0000
S(1)	0.1225(5)	0.0625(5)	−0.0899(5)
Cu(1)	−0.0606(2)	−0.1859(2)	−0.0000(1)
Cl(1)	−0.1111(5)	−0.3379(4)	−0.0000(1)
N(1)	0.5000	0.0000	−0.2500
C(11)	0.463(1)	0.083(1)	−0.1810(9)
C(12)	0.428(1)	0.171(1)	−0.236(1)
C(13)	0.380(2)	0.232(2)	−0.152(3)
C(14)	0.383(3)	0.318(3)	0.835(3)

Table 3 Selected interatomic distances (Å) and angles (°) for compound **1a**

Mo–S(1)	2.230(6)	Cu(1)–S(1)	2.242(7)
Mo ··· Cu(1)	2.609(2)	Cu(1)–Cl(1)	2.136(5)
S(1)–Mo–S(1)	108.9(2)	S(1)–Cu(1)–Mo	54.1(2)
Cu(1)–Mo–S(1)	125.6(2)	Cl(1)–Cu(1)–Mo	179.7(2)
Cu(1)–Mo–Cu(1)	90.0(4)	S(1)–Cu(1)–S(1)	108.2(3)
Cu(1)–S(1)–Mo	71.5(2)	Cl(1)–Cu(1)–S(1)	125.6(2)
Cu(1)–S(1)–Cu(1)	111.0(3)		

$[NPr_4]_2[MoS_4Cu_4Cl_4]$ **3a**. Copper(I) chloride (200 mg, 2 mmol) was added with stirring to a solution (60 cm^3) of $[NPr_4]_2[MoS_4]$ (298 mg, 0.5 mmol) in dichloromethane. After stirring for 18 h at room temperature the mixture was filtered and the filtrate reduced to *ca.* 25 cm^3 under reduced pressure. Violet crystals were obtained (yield 60 mg, 12%) [Found (Calc. for $C_{24}H_{56}Cl_4Cu_4MoN_2S_4$): C, 29.20 (29.05); H, 5.75 (5.65); Cl, 14.05 (14.30); Cu, 24.70 (25.60); Mo, 9.70 (9.70); N, 2.95 (2.80); S, 12.65 (12.90%)].

$[NPr_4]_2[WS_4Cu_4Cl_4]$ **3b**. Copper(I) chloride (200 mg, 2 mmol) was added with stirring to a solution (60 cm^3) of $[NPr_4]_2[WS_4]$ (340 mg, 0.5 mmol) in dichloromethane. After stirring for 30 min at room temperature the orange-red mixture was filtered to eliminate a red solid. Addition of Et_2O (*ca.* 10 cm^3) gave after 24 h orange crystals (yield 80 mg, 15%) [Found (Calc. for $C_{24}H_{56}Cl_4Cu_4N_2S_4W$): C, 27.40 (26.65); H, 5.45 (5.20); Cl, 13.30 (13.15); Cu, 22.90 (23.50); N, 2.70 (2.60); S, 11.05 (11.85); W, 17.75 (17.05%)].

Crystal-structure Determinations. Unit-cell parameters for compounds **1a**, **2** and **3b** were obtained from least-squares refinement of the positions of 25 reflections. Intensity data were collected at room temperature with a θ–2θ scan technique and a variable speed. They were corrected for Lorentz and polarization effects. For compounds **1a** and **2** an empirical absorption correction based on the DIFABS program[11] was applied; for **3b** the ψ-scan technique was used. The structures of **2** and **3b** were solved by the heavy-atom method, **1a** by direct methods.[12] After location of metallic centres the positions of the remaining non-hydrogen atoms were obtained from subsequent Fourier maps. All atom parameters were refined anisotropically,[13] hydrogen contributions being omitted. Calculations were performed with a MicroVax II computer. Specific parameters pertaining to data collection are reported in Table 1.

Additional material available from the Cambridge Crystallographic Data Centre comprises thermal parameters and remaining bond lengths and angles.

Results

$[NBu_4]_2[MoS_4Cu_4Cl_4]$ **1a**. Fractional atomic coordinates and interatomic distances and angles are given in Tables 2 and 3.

Table 4 Fractional atomic coordinates for $[PPh_4][NPr_4][MoS_4Cu_4Cl_4]$ **2**

Atom	*X/a*	*Y/b*	*Z/c*
Mo(1)	0.018 71(9)	0.100 36(2)	0.635 35(7)
S(1)	0.027 1(3)	0.092 29(8)	0.469 0(2)
S(2)	0.184 8(3)	0.139 44(7)	0.719 7(2)
S(3)	−0.189 4(3)	0.123 2(1)	0.632 6(2)
S(4)	0.055 2(4)	0.047 75(8)	0.720 9(2)
Cu(1)	0.213 7(1)	0.086 95(3)	0.808 48(9)
Cu(2)	−0.184 0(1)	0.112 97(5)	0.464 6(1)
Cu(3)	0.048 8(2)	0.037 36(4)	0.549 3(1)
Cu(4)	−0.024 6(2)	0.163 43(4)	0.709 2(1)
Cl(1)	0.364 7(3)	0.073 70(8)	0.953 8(2)
Cl(2)	−0.351 4(3)	0.123 8(1)	0.325 9(2)
Cl(3)	0.181 8(2)	−0.004 50(8)	0.500 6(2)
Cl(4)	−0.056 2(5)	0.217 2(1)	0.755 1(3)
N(1)	0.104(1)	0.494 8(3)	0.271(1)
C(1)	0.008(1)	0.506 7(4)	0.335(1)
C(2)	−0.115(2)	0.529 8(6)	0.274(1)
C(3)	−0.211(2)	0.538 2(6)	0.345(2)
C(4)	0.034(3)	0.471 4(6)	0.178(1)
C(5)[a]	−0.012(3)	0.442 0(8)	0.197(2)
C(6)[a]	−0.055(4)	0.422 2(9)	0.083(3)
C(7)[a]	0.132(3)	0.523 5(7)	0.204(2)
C(8)[a]	0.213(4)	0.554(1)	0.282(4)
C(9)[a]	0.271(4)	0.584 5(9)	0.225(4)
C(10)	0.220(2)	0.475 6(5)	0.348(2)
C(11)	0.232(5)	0.443(1)	0.359(2)
C(12)	0.365(3)	0.427 3(9)	0.446(2)
C(51)[b]	0.055(3)	0.451 5(8)	0.095(2)
C(61)[b]	−0.036(4)	0.426(1)	0.029(3)
C(71)[b]	0.223(4)	0.528(1)	0.253(3)
C(81)[b]	0.295(5)	0.546(2)	0.332(4)
C(91)[b]	0.374(5)	0.578(1)	0.276(5)
P(1)	−0.089 2(3)	0.221 36(8)	0.123 1(2)
C(101)	−0.107(1)	0.226 1(3)	0.255 9(9)
C(102)	−0.062(2)	0.200 3(4)	0.331(1)
C(103)	−0.074(2)	0.204 2(5)	0.432(1)
C(104)	−0.127(2)	0.236 4(5)	0.461(1)
C(105)	−0.167(3)	0.262 8(7)	0.387(1)
C(106)	−0.156(2)	0.257 6(5)	0.287(1)
C(107)	−0.230(1)	0.195 9(3)	0.041 7(9)
C(108)	−0.292(1)	0.169 6(4)	0.090(1)
C(109)	−0.393(2)	0.146 6(5)	0.020(2)
C(110)	−0.428(2)	0.152 6(6)	−0.089(2)
C(111)	−0.362(2)	0.178 6(5)	−0.135(1)
C(112)	−0.260(1)	0.201 2(4)	−0.067(1)
C(113)	−0.082(1)	0.265 0(3)	0.064 2(8)
C(114)	0.034(1)	0.276 2(4)	0.039(1)
C(115)	0.043(2)	0.309 7(5)	−0.010(2)
C(116)	−0.067(2)	0.331 5(4)	−0.027(1)
C(117)	−0.191(2)	0.321 5(5)	−0.005(1)
C(118)	−0.206(2)	0.285 7(4)	0.038(1)
C(119)	0.067(1)	0.198 0(3)	0.127 0(8)
C(120)	0.067(1)	0.170 6(4)	0.056(1)
C(121)	0.197(2)	0.152 1(5)	0.058(2)
C(122)	0.315(2)	0.163 4(5)	0.133(1)
C(123)	0.315(1)	0.190 5(5)	0.204(1)
C(124)	0.191(1)	0.208 5(3)	0.202(1)

[a] Occupancy 0.6. [b] Occupancy 0.4.

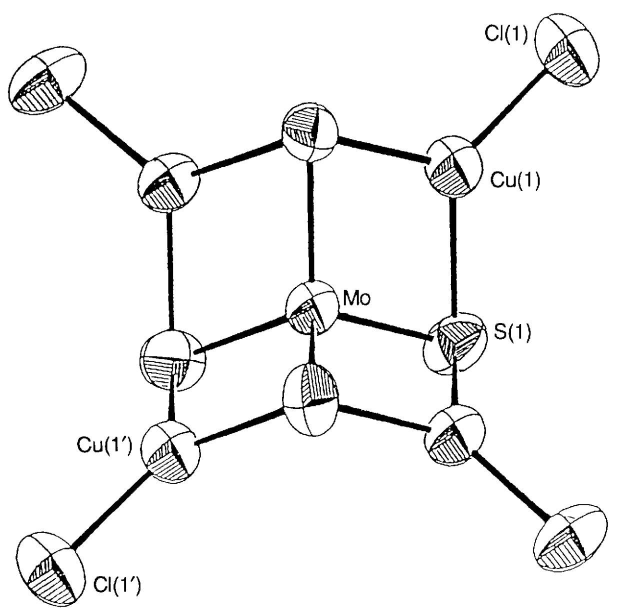

Fig. 1 An ORTEP drawing of the discrete $[MoS_4Cu_4Cl_4]^{2-}$ anion

The structure of compound **1a** consists of a discrete $[MoS_4Cu_4Cl_4]^{2-}$ independent dianion and two $[NBu_4]^+$ cations. The shortest non-bonding Cu ··· Cl distance between $MoS_4Cu_4Cl_4$ aggregates is 5.41 Å. The pentanuclear anion is represented in Fig. 1. The $MoS_4Cu_4Cl_4$ core is generated by the $\bar{4}$ axis passing through the Mo located at the origin giving an idealized sulphur tetrahedron, angles S–Mo–S are 108.9(2)°. The copper atoms are three-co-ordinated with a trigonal-planar environment imposed by symmetry. The four MoS_2CuCl units are strictly planar with four short terminal Cu–Cl distances of 2.136(5) Å as expected for discrete units.

Table 5 Selected interatomic distances (Å) and angles (°) for compound **2**

Mo(1)–S(1)	2.225(3)	Mo(1)–S(2)	2.248(3)
Mo(1)–S(3)	2.230(3)	Mo(1)–S(4)	2.225(3)
Mo(1) ··· Cu(1)	2.605(1)	Mo(1) ··· Cu(2)	2.619(2)
Mo(1) ··· Cu(3)	2.639(2)	Mo(1) ··· Cu(4)	2.604(2)
S(1)–Cu(2)	2.224(3)	S(1)–Cu(3)	2.270(3)
S(2)–Cu(1)	2.240(3)	S(2)–Cu(4)	2.236(3)
S(3)–Cu(2)	2.250(3)	S(3)–Cu(4)	2.240(4)
S(4)–Cu(1)	2.220(3)	S(4)–Cu(3)	2.267(3)
Cu(1)–Cl(1)	2.140(3)	Cu(2)–Cl(2)	2.146(3)
Cu(3)–Cl(3)	2.239(3)	Cu(3)–Cl(3)	2.523(3)
Cu(4)–Cl(4)	2.123(4)		
S(2)–Mo(1)–S(1)	110.5(1)	S(4)–Mo(1)–S(1)	109.5(1)
S(3)–Mo(1)–S(1)	108.5(1)	S(4)–Mo(1)–S(2)	108.4(1)
S(3)–Mo(1)–S(2)	108.8(1)	S(4)–Mo(1)–S(3)	111.3(1)
Cu(2)–S(1)–Mo(1)	72.1(1)	Cu(1)–S(2)–Mo(1)	70.95(9)
Cu(3)–S(1)–Mo(1)	71.90(9)	Cu(4)–S(2)–Mo(1)	70.99(9)
Cu(2)–S(3)–Mo(1)	71.5(1)	Cu(1)–S(4)–Mo(1)	71.76(9)
Cu(4)–S(3)–Mo(1)	71.3(1)	Cu(3)–S(4)–Mo(1)	71.97(9)
Cu(3)–S(1)–Cu(2)	106.9(1)	Cu(4)–S(3)–Cu(2)	110.0(1)
Cu(4)–S(2)–Cu(1)	111.2(1)	Cu(3)–S(4)–Cu(1)	116.7(1)
Cl(1)–Cu(1)–S(2)	128.4(1)	Cl(1)–Cu(1)–S(4)	122.8(1)
S(4)–Cu(1)–S(2)	108.8(1)		
Cl(2)–Cu(2)–S(1)	126.7(1)	Cl(2)–Cu(2)–S(3)	125.4(1)
S(3)–Cu(2)–S(1)	107.8(1)		
Cl(3)–Cu(3)–S(1)	118.3(1)	Cl(3)–Cu(3)–S(4)	122.7(1)
Cl(3)–Cu(3)–S(1)	110.1(1)	Cl(3)–Cu(3)–S(4)	96.8(1)
S(4)–Cu(3)–S(1)	106.4(1)		
Cl(3)–Cu(3)–Cl(3)	99.26(9)		
Cl(4)–Cu(4)–S(2)	124.1(2)	Cl(4)–Cu(4)–S(3)	126.9(2)
S(3)–Cu(4)–S(2)	108.8(1)		

$[PPh_4][NPr_4][MoS_4Cu_4Cl_4]$ **2**.—Positional atomic co-ordinates are given in Table 4 and selected geometrical parameters in Table 5. The structure determination confirms the 4:1 Cu:Mo stoichiometry. The inversion centre generates the $[Mo_2S_8Cu_8Cl_8]^{4-}$ dimer represented in Fig. 2. Atoms Cu(1), Cu(2) and Cu(4) display a trigonal-planar geometry with Cl–Cu–S angles ranging from 122.76(13) to 128.41(12)° and three short terminal Cu–Cl distances of 2.123(4)–2.146(3) Å. The geometry at the Cu(3) atom is distorted tetrahedral with angles in the range 97.77(12)–122.72(13)°. As expected the Cu(3)–Cl distances at the (μ-Cl)$_2$ bridge are longer than the terminal ones, 2.239(9)–2.523(3) Å. In the $[NPr_4]^+$ cation atoms C(5), C(6), C(7), C(8) and C(9) are disordered. Disordered positions C(51)–C(91) were obtained from Fourier-difference maps. The refinements of occupancy factors converged respectively to 0.6 and 0.4, see Table 4.

$[NPr_4]_2[WS_4Cu_4Cl_4]$ **3b**.—Final positional parameters are given in Table 6 and selected interatomic distances and angles in Table 7. The structure of compound **3b** consists of $[WS_4Cu_4Cl_4]^{2-}$ anion and $[NPr_4]^+$ cations. The inversion centre generates an anionic polymeric chain running along a direction parallel to the [0 1 1] axis as shown in Fig. 3. Atoms Cu(1) and Cu(2) have a trigonal-planar geometry, with Cl–Cu–S angles ranging from 123.61(8) to 129.21(6)° and short terminal distances Cu(1)–Cl(1) 2.144(1) Å and Cu(2)–Cl(2) 2.160(1) Å. In the $WS_4Cu_4Cl_4$ core the two atoms Cu(3) and Cu(4) have a distorted-tetrahedral geometry; atoms Cl(3) and Cl(4) serve as links between $WS_4Cu_4Cl_4$ units to form the infinite chain represented in Fig. 3. One of the two crystallographically independent $[NPr_4]^+$ cations is disordered. Two different positions C(62), C(63), C(72) and C(62′), C(63′), C(72′) were located in the Fourier-difference map. Refined occupancy factors of the two sites converged respectively to 0.66 and 0.34.

Discussion

Crystal Structures.—Compound **1a**. For a crystallographic reason $[MoS_4Cu_4Cl_4]^{2-}$ **1a** is symmetrical. The five atoms Cl(1), Cu(1), Mo, Cu(1′) and Cl(1′) lie on a straight line, angle Cl(1)–Cu(1)–Mo 179.7(2)° and the MoS(1)Cu(1)S(1) moiety is planar. In this plane the Mo $\cdots$ Cu(1) distance is very short, 2.609(2) Å, actually the shortest metal–metal separation encountered in this type of compound. Extended-Hückel calculations were performed to evaluate roughly the interaction between the two close metals. The MoS(1)S(1)Cu(1)Cl(1) unit was built up from the MoS_4 and CuCl fragments in a system of internal coordinates centred on the molybdenum, with Cu(1) located 2.25 Å from sulphur with an angle of 72.4°, and Cl(1) at 2.14 Å from copper with an angle of 120° in an idealized geometry. One of the orbitals which describe the MoS(1)Cu(1)Cl(1) fragment is constituted of an admixture of a $[-(d_{x^2-y^2}) - d_{z^2}] = d_{y^2}$ orbital of copper with the d_{z^2} of molybdenum as shown. The direct overlap between metallic orbitals is accompanied by a contribution from sulphur p orbitals, (*i*) non-bonding with Mo, (*ii*) antibonding with copper.

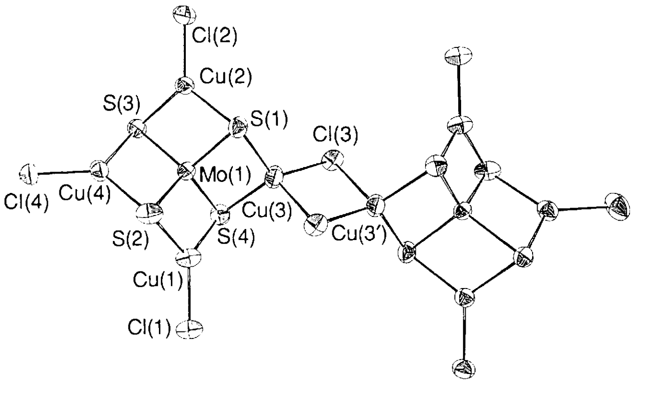

Fig. 2 An ORTEP drawing of the $[Mo_2S_8Cu_8Cl_8]^{4-}$ dimer

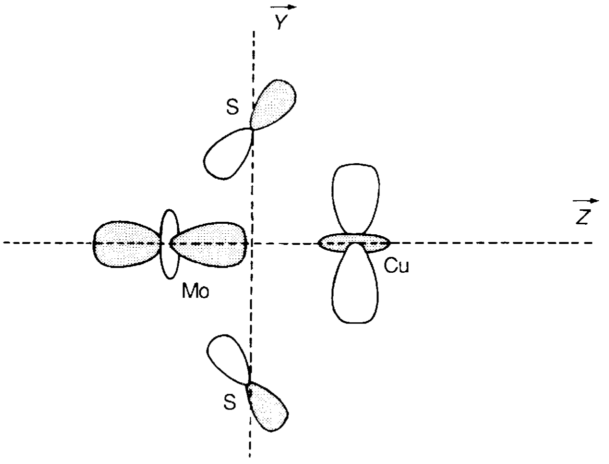

Table 6 Fractional atomic coordinates for $[NPr_4]_2[WS_4Cu_4Cl_4]$ **3b**

Atom	*X/a*	*Y/b*	*Z/c*
W(1)	−0.053 55(2)	0.234 91(1)	0.254 09(1)
S(1)	−0.068 0(1)	0.233 62(9)	0.399 73(8)
S(2)	−0.219 0(1)	0.105 58(9)	0.159 65(7)
S(3)	0.143 2(1)	0.207 70(9)	0.204 27(9)
S(4)	−0.071 6(1)	0.391 29(9)	0.251 87(8)
Cu(1)	0.121 07(6)	0.359 79(5)	0.192 02(5)
Cu(2)	−0.232 04(6)	0.100 99(4)	0.305 33(4)
Cu(3)	−0.020 00(6)	0.077 10(5)	0.101 19(4)
Cu(4)	−0.061 89(7)	0.402 35(5)	0.405 69(4)
Cl(1)	0.259 7(2)	0.448 2(1)	0.128 3(1)
Cl(2)	−0.377 2(1)	−0.007 3(1)	0.348 3(1)
Cl(3)	0.030 1(1)	−0.084 17(9)	0.054 38(9)
Cl(4)	−0.171 1(1)	0.504 8(1)	0.511 18(9)
N(1)	−0.381 6(4)	0.259 7(3)	−0.046 1(3)
C(1)	−0.503 6(5)	0.251 6(4)	−0.106 2(4)
C(2)	−0.360 6(5)	−0.207 3(5)	0.078 1(4)
C(3)	−0.251 7(6)	−0.211 7(5)	0.144 2(6)
C(11)	−0.382 8(5)	0.330 5(4)	0.054 4(3)
C(12)	−0.391 0(6)	0.442 8(4)	0.068 5(4)
C(13)	−0.375 3(8)	0.505 5(5)	0.172 6(5)
C(21)	−0.376 2(5)	0.152 1(4)	−0.042 6(3)
C(22)	−0.371 0(6)	0.066 9(4)	−0.135 1(4)
C(23)	−0.388 9(6)	−0.038 6(4)	−0.120 3(5)
C(31)	−0.260 8(5)	0.302 0(4)	−0.090 2(4)
C(32)	−0.126 3(5)	0.330 8(4)	−0.032 9(5)
C(33)	−0.019 3(6)	0.360 8(6)	−0.092 7(6)
N(2)	0.379 8(4)	0.223 0(3)	0.492 3(3)
C(41)	0.271 2(6)	0.276 6(5)	0.539 9(5)
C(42)	0.205 9(9)	0.233 1(8)	0.610 9(6)
C(43)	0.098 0(8)	0.296 8(8)	0.650 2(6)
C(51)	0.324 1(7)	0.105 1(5)	0.445 0(5)
C(52)	0.200 4(9)	0.069 4(7)	0.377 4(7)
C(53)	0.140(1)	−0.047 5(9)	0.344 4(9)
C(61)	0.418 0(6)	0.271 1(6)	0.419 2(5)
C(62)[a]	0.532 1(9)	0.251 4(8)	0.361 2(6)
C(63)[a]	0.549(1)	0.320(1)	0.300 7(8)
C(71)	0.494 6(7)	0.234 1(7)	0.555 7(5)
C(72)[a]	0.587 8(9)	0.335 7(7)	0.611 1(7)
C(73)	0.711 1(9)	0.308(1)	0.646 8(6)
C(62′)[b]	0.481(2)	0.382 9(9)	0.438(1)
C(63′)[b]	0.525(2)	0.384(2)	0.343(1)
C(72′)[b]	0.641(1)	0.245(2)	0.549 0(9)

[a] Occupancy 0.66. [b] Occupancy 0.34.

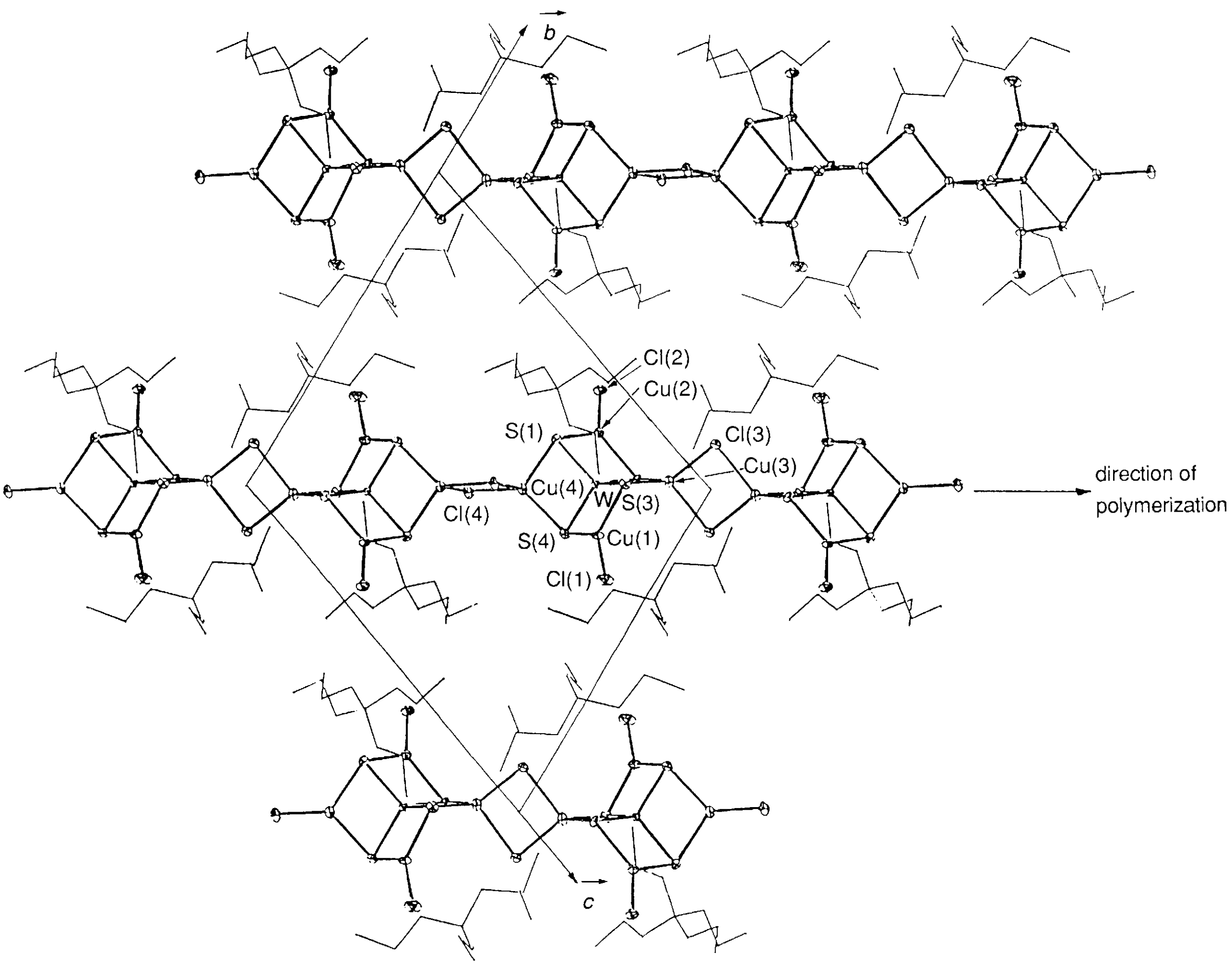

Fig. 3 An ORTEP drawing of $[NPr_4]_2[WS_4Cu_4Cl_4]$ showing the chains. Thermal ellipsoids of cations were omitted for clarity

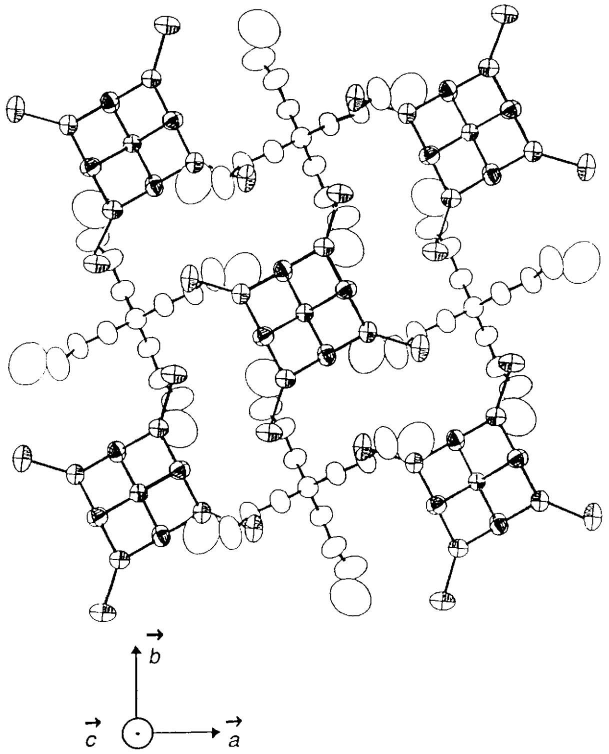

Fig. 4 View of the packing of $[NBu_4]_2[MoS_4Cu_4Cl_4]$

In the solid state, the $MoS_4Cu_4Cl_4$ units are well separated by $[NBu_4]^+$ cations as shown in Fig. 4. Interations between $[MoS_4Cu_4Cl_4]^{2-}$ anions are screened by cations, producing the ideal tetrahedral geometry of the central MoS_4Cu_4 core with a short Mo $\cdots$ Cu distance.

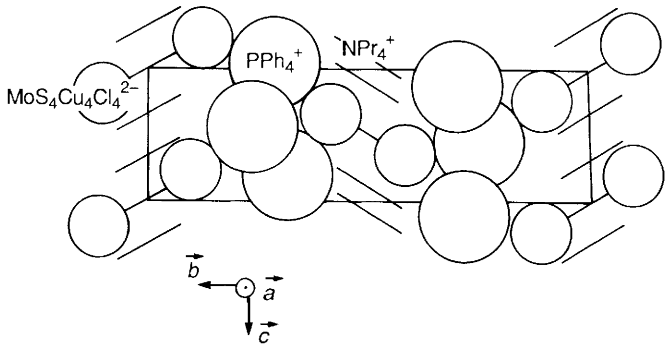

Fig. 5 Schematic diagram representing the packing of $[NPr_4][PPh_4]$-$[MoS_4Cu_4Cl_4]$

Compound **2**. In contrast, strong interactions between $[MoS_4Cu_4Cl_4]^{2-}$ anions exist for compound **2** that lead to $[Mo_2S_8Cu_8Cl_8]^{4-}$ dimers. The Cu(3) $\cdots$ Cu(3′) distance equal to 3.092 Å is very short, whereas the Mo(1)–Cu(3) distance separation is long, 2.639 Å, close to values observed for compound **1a**, see Table 8. The packing of **2** is represented in Fig. 5 as a schematic diagram. The $Mo_2S_8Cu_8Cl_8$ units are alternately stacked with $[NPr_4]^+$ cations and the oversized $[PPh_4]^+$ cations located between stacks preclude any association between $Mo_2S_8Cu_8Cl_8$ groups.

Compound **3b**. Association between $W_2S_8Cu_8Cl_8$ units through chloro-bridges were obtained by replacing the hindering $[PPh_4]^+$ by $[NPr_4]^+$ cations. The polyanion

Table 7 Selected interatomic distances (Å) and angles (°) for compound **3b**

W(1)–S(1)	2.233(1)	W(1)–S(2)	2.243(1)
W(1)–S(3)	2.231(1)	W(1)–S(4)	2.237(1)
W(1) ··· Cu(1)	2.6408(6)	W(1) ··· Cu(2)	2.6495(6)
W(1) ··· Cu(3)	2.6777(6)	W(1) ··· Cu(4)	2.6710(6)
S(1)–Cu(2)	2.254(1)	S(1)–Cu(4)	2.307(1)
S(2)–Cu(2)	2.249(1)	S(2)–Cu(3)	2.299(1)
S(3)–Cu(1)	2.248(1)	S(3)–Cu(3)	2.287(1)
S(4)–Cu(1)	2.255(1)	S(4)–Cu(4)	2.295(1)
Cu(1)–Cl(1)	2.144(1)	Cu(2)–Cl(2)	2.160(1)
Cu(3)–Cl(3)	2.283(1)	Cu(3)–Cl(3)	2.410(1)
Cu(4)–Cl(4)	2.241(1)	Cu(4)–Cl(4)	2.544(1)
S(2)–W(1)–S(1)	108.11(4)	S(3)–W(1)–S(1)	110.55(5)
S(3)–W(1)–S(2)	109.41(4)	S(4)–W(1)–S(1)	109.80(4)
S(4)–W(1)–S(2)	110.61(5)	S(4)–W(1)–S(3)	108.37(4)
Cu(2)–S(1)–W(1)	72.39(4)	Cu(4)–S(1)–W(1)	72.06(4)
Cu(2)–S(2)–W(1)	72.31(4)	Cu(3)–S(2)–W(1)	72.25(4)
Cu(1)–S(3)–W(1)	72.25(4)	Cu(3)–S(3)–W(1)	72.68(4)
Cu(1)–S(4)–W(1)	72.01(4)	Cu(4)–S(4)–W(1)	72.21(4)
Cu(3)–S(3)–Cu(1)	106.59(5)	Cu(4)–S(4)–Cu(1)	109.31(5)
Cu(4)–S(1)–Cu(2)	118.23(5)	Cu(3)–S(2)–Cu(2)	112.50(5)
Cl(1)–Cu(1)–S(3)	123.61(6)	Cl(1)–Cu(1)–S(4)	129.21(6)
S(4)–Cu(1)–S(3)	107.13(5)		
Cl(2)–Cu(2)–S(1)	126.12(5)	Cl(2)–Cu(2)–S(2)	126.69(5)
S(2)–Cu(2)–S(1)	107.17(4)		
Cl(3)–Cu(3)–S(3)	113.83(5)	Cl(3)–Cu(3)–S(2)	122.84(5)
Cl(3)–Cu(3)–S(3)	113.11(5)	Cl(3)–Cu(3)–S(2)	106.44(5)
Cl(3)–Cu(3)–Cl(3)	94.75(4)	S(3)–Cu(3)–S(2)	105.57(4)
Cl(4)–Cu(4)–S(1)	120.47(5)	Cl(4)–Cu(4)–S(4)	121.22(5)
Cl(4)–Cu(4)–S(1)	99.73(5)	Cl(4)–Cu(4)–S(4)	111.25(5)
Cl(4)–Cu(4)–Cl(4)	96.13(4)	S(4)–Cu(4)–S(1)	105.23(5)
Cu(3)–Cl(3)–Cu(3)	85.25(4)	Cu(4)–Cl(4)–Cu(4)	83.87(4)

Table 8 Intermetallic distances (Å)

	M ··· Cu		
Compound	Cu-(trigonal)	Cu(tetra-gonal)	Cu ··· Cu
1a $[NBu_4]_2[MoS_4Cu_4Cl_4]$	2.609	—	—
2 $[PPh_4][NPr_4][MoS_4Cu_4Cl_4]$	2.609	2.639	3.092
3b $[NPr_4]_2[WS_4Cu_4Cl_4]$	2.645	2.674	3.192
$[PPh_4]_2[WS_4Cu_4Cl_4]$[7]	2.635	2.675	—

structure is linear, Fig. 3, and the anion–cation stacking observed for **2** is retained. Along the [0 1 1] direction of polymerization, the W ··· Cu(tetragonal) and Cu(tetragonal) ··· Cu(tetragonal) distances increased to reach respectively the mean values of 2.674 and 3.197 Å. For compound **3b**, a long W ··· Cu distance of 2.645 Å is observed. The same type of separation is significantly shorter in compounds **1a** and **2**, see Table 8. This difference is related to the number of Cu(trigonal) present in the compound: **1a** contains four equivalent Cu(trigonal), **2** three Cu(trigonal) and one Cu(tetragonal) and **3b** two Cu(trigonal) and two Cu(tetragonal).

The short Cu(3) ··· Cu(3′) distance observed in compound **2** is probably a consequence of steric effects since the anion is blocked between two $[PPh_4]^+$ cations rather than to electronic effects. This assumption is confirmed by the lengthening of the analogous Cu(3) ··· Cu(3′) and Cu(4) ··· Cu(4′) distances observed in the polymer when replacing $[PPh_4]^+$ by $[NPr_4]^+$.

Another effect due to the size of the cation on the dimensionality of the structures was observed with NCS^- ligands bonded to copper.[9,10] The chemical analogues $[WS_4Cu_4(NCS)_4]^{2-}$ were isolated as one-, two- and three-dimensional arrays by varying the cation size associated with the anionic group. With chloro-ligands, only chain or discrete compounds were isolated owing to the weaker bridging ability of the chlorides compared to the NCS^- ambidentate ligands.

Table 9 Spectral data for the complexes

	IR[a]/cm^{-1}		
Compound	ν(M–S)	ν(Cu–Cl)	UV/VIS[b]
$[NBu_4]_2[MoS_4Cu_4Cl_4]$ **1a**	460s	350s	520 (2.9), 368 (sh), 290 (21.6)
$[PPh_4][NPr_4][MoS_4Cu_4Cl_4]$ **2**	460s	350m	516 (2.4), 368 (sh)
$[NPr_4]_2[MoS_4Cu_4Cl_4]$ **3a**	450s	350m	512 (2.7), 368 (sh)
$[NBu_4]_2[WS_4Cu_4Cl_4]$ **1b**	445s	355s	442 (3.8), 330 (sh), 306 (sh)
$[NPr_4]_2[WS_4Cu_4Cl_4]$ **3b**	445s	340m	440 (3.4), 330 (sh), 304 (sh)
$[PPh_4]_2[WS_4\{Cu(NCS)\}_4]$			430 (4.4), 320 (sh)
$[NEt_4]_2[WS_4\{Cu(NCS)\}_4]$			430 (4.69), 320 (sh)
$[NMe_4]_2[WS_4\{Cu(NCS)\}_4]$			430 (4.48), 320 (sh)
$[PPh_4]_2[MoS_4\{Cu(NCS)\}_4]$			510 (3.05), 360 (sh)
$[NEt_4]_2[MoS_4\{Cu(NCS)\}_4]$			510 (3.00), 360 (sh)
$[NMe_4]_2[MoS_4\{Cu(NCS)\}_4]$			510 (3.30), 360 (sh)

[a] s = Strong, m = medium. [b] Wavelength (nm), molar absorption (10^{-3} dm^3 mol^{-1} cm^{-1}).

Infrared Spectra.—In the 400–500 cm^{-1} region where ν(M–S) frequencies are expected[16,17] all compounds exhibit only one band consistent with the symmetry of the MS_4Cu_4 core given from X-ray data. In the 300–360 cm^{-1} region, where ν(Cu–Cl) are generally observed,[17] the spectra of the various compounds are different, see Table 9. For compounds **1a** and **1b** a strong band is observed at 350 cm^{-1} corresponding to the stretching mode of the four equivalent terminal Cu(trigonal)Cl groups. For compound **2** the intensity of the band at 350 cm^{-1} decreased because of the presence of only three terminal Cu(trigonal)Cl groups, the fourth CuCl group being engaged in the μ-chloro-bridge. For compounds **3a** and **3b** the intensity of the band at 350 cm^{-1} is yet weaker because only two copper atoms have trigonal geometry and since the two others are engaged in two chloro-bridges.

Electronic Spectra.—Electronic spectral data for the $[MS_4Cu_4X_4]^{2-}$ anions, M = Mo or W and X = Cl^- or NCS^-, are given in Table 9. Main absorptions are attributed to the charge-transfer transitions of the MS_4 core.[18–20] For X = NCS^-, electronic spectra in solution were similar in profile, wavelength and intensity, independent of polymerization in the solid state. This looks to be convincing spectroscopic evidence that the various polymeric structures cleaved in dmf solutions to give the same absorbing species. Solutions are stable, no change in absorption being observed for aged solutions. In contrast, the spectra of chloro-species are different. The positions of the absorption peak vary from 520 nm for the molybdenum monomer to 512 nm for the polymer showing that solutions do not contain the same absorbing species. Furthermore, the resulting solutions are not stable and on ageing tend to form colloidal systems. Light-scattering and electronic microscopy measurements are in progress to elucidate the nature and size of the particles.

References

1 (*a*) A. Müller, M. Dartmann, C. Romer, W. Clegg and G. Sheldrick, *Angew. Chem., Int. Ed. Engl.*, 1981, **20**, 1060; (*b*) S. F. Gheller, T. W. Hambley, J. R. Rodgers, R. T. C. Brownlee, M. J. O'Connors, M. R. Snow and A. Wedd, *Inorg. Chem.*, 1984, **23**, 2519.

2 F. Sécheresse, M. Salis, C. Potvin and J. M. Manoli, *Inorg. Chim. Acta*, 1986, 114, L19.

3 J. M. Manoli, C. Potvin and F. Sécheresse, *J. Chem. Soc., Chem. Commun.*, 1982, 1159.

4 W. Clegg, C. D. Garner and J. R. Nicholson, *Acta Crystallogr., Sect. C*, 1983, **39**, 552.

5 F. Sécheresse, J. M. Manoli, C. Potvin and S. Marzak, *J. Chem. Soc., Dalton Trans.*, 1988, 3055.

6 J. R. Nicholson, A. C. Flood, C. D. Garner and W. Clegg, *J. Chem. Soc., Chem. Commun.*, 1983, 1179.

7 W. Clegg, C. D. Scattergood and C. D. Garner, *Acta Crystallogr., Sect. C*, 1987, **43**, 786.

8 J. M. Manoli, C. Potvin, F. Sécheresse and S. Marzak, *J. Chem. Soc., Chem. Commun.*, 1986, 1557.

9 C. Potvin, J. M. Manoli, F. Secheresse and S. Marzak, *Inorg. Chem.*, 1987, **26**, 4370.

10 J. M. Manoli, C. Potvin, F. Sécheresse and S. Marzak, *Inorg. Chim. Acta*, 1988, **150**, 257.

11 N. Walker and D. Stuart, *Acta Crystallogr., Sect. A*, 1983, **39**, 158.

12 G. M. Sheldrick, SHELX 86, a program for crystal structure determination, University of Göttingen, 1986.

13 D. J. Watkin, J. K. Carruthers and P. W. Betteridge, CRYSTALS, An Advanced Crystallographic Program System, Chemical Crystallography Laboratory, University of Oxford, 1988.

14 *International Tables for X-Ray Crystallography*, Kynoch Press, Birmingham, 1974, vol. 4.

15 A. C. Larsen, *Crystallographic Computing*, Munksgaard, Copenhagen, 1970, p. 291.

16 A. Müller, W. Jaegermann and W. Hellmann, *J. Mol. Struct.*, 1983, **100**, 559.

17 R. J. H. Clark, S. Joss, M. Zragulis, C. D. Garner and J. R. Nicholson, *J. Chem. Soc., Dalton Trans.*, 1986, 1595.

18 A. Müller, E. Diemann, R. Jostes and H. Bögge, *Angew. Chem., Int. Ed. Engl.*, 1981, **20**, 934.

19 R. J. H. Clark, T. J. Dimes and M. L. J. Wolf, *J. Chem. Soc., Faraday Trans. 2*, 1982, 679.

20 R. J. H. Clark, T. J. Dimes and G. P. Proud, *J. Chem. Soc., Dalton Trans.*, 1983, 2019.

Received 15*th February* 1991; *Paper* 1/00741F